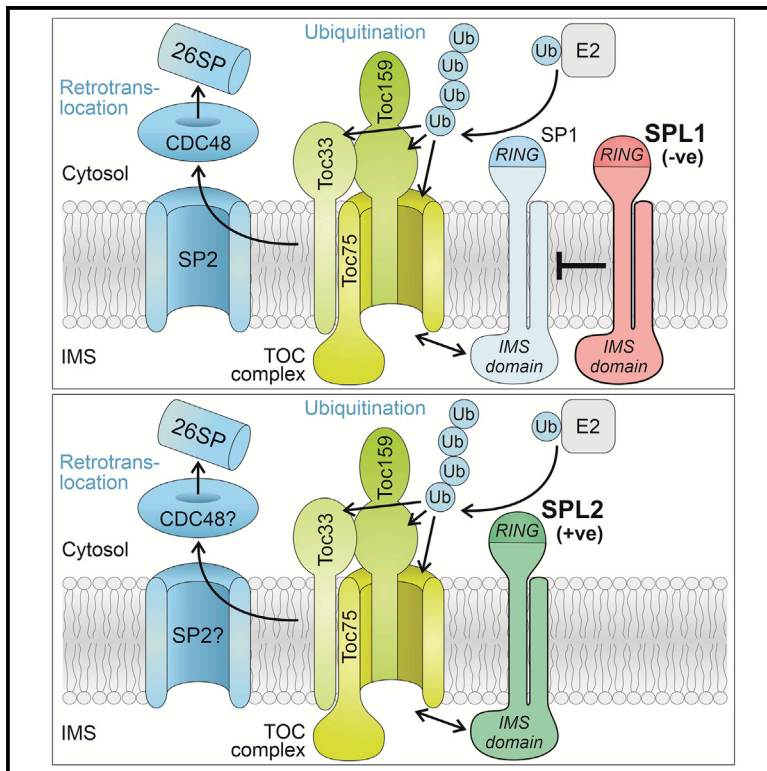


Current Biology

Multiple ubiquitin E3 ligase genes antagonistically regulate chloroplast-associated protein degradation

Graphical abstract



Authors

Sabri Mohd. Ali, Na Li, Ziad Soufi, Jinrong Yao, Errin Johnson, Qihua Ling, R. Paul Jarvis

Correspondence

paul.jarvis@biology.ox.ac.uk

In brief

Mohd. Ali et al. study SPL1 and SPL2, homologs of ubiquitin E3 ligase SP1, which mediates chloroplast-associated protein degradation (CHLORAD). SPL1 negatively regulates SP1, whereas SPL2 shares redundancy with SP1. Both homologs affect leaf senescence, but in diametrically opposite ways. Thus, multiple E3 genes antagonistically regulate CHLORAD.

Highlights

- SPL1 and SPL2 are chloroplast SP1 homologs that appeared early in plant evolution
- SPL1 negatively regulates SP1, potentially interfering with its E3 ligase activity
- SPL2, the more divergent SP1 homolog, shares functional redundancy with SP1
- SPL1 and SPL2 affect leaf senescence, similar to SP1, but in diametrically opposite ways



Report

Multiple ubiquitin E3 ligase genes antagonistically regulate chloroplast-associated protein degradation

Sabri Mohd. Ali,^{1,5} Na Li,^{1,6} Ziad Soufi,^{1,6} Jinrong Yao,^{2,4} Errin Johnson,³ Qihua Ling,^{1,4} and R. Paul Jarvis^{1,7,*}

¹Section of Molecular Plant Biology (Department of Biology) and Department of Plant Sciences, University of Oxford, South Parks Road, Oxford OX1 3RB, UK

²University of Chinese Academy of Sciences, Beijing 100049, China

³The Sir William Dunn School of Pathology, University of Oxford, Oxford OX1 3RE, UK

⁴National Key Laboratory of Plant Molecular Genetics, CAS Centre for Excellence in Molecular Plant Sciences, Institute of Plant Physiology and Ecology, Chinese Academy of Sciences, Shanghai 200032, China

⁵Present address: Environmental and Life Sciences Programme, Faculty of Science, Universiti Brunei Darussalam, Bandar Seri Begawan BE1410, Brunei Darussalam

⁶These authors contributed equally

⁷Lead contact

*Correspondence: paul.jarvis@biology.ox.ac.uk

<https://doi.org/10.1016/j.cub.2023.01.060>

SUMMARY

The chloroplast is the most prominent member of a diverse group of plant organelles called the plastids, and it is characterized by its vital role in photosynthesis.^{1–3} Most of the ~3,000 different proteins in chloroplasts are synthesized in the cytosol in precursor (preprotein) form, each with a cleavable transit peptide.^{4–8} Preproteins are imported via translocons in the outer and inner envelope membranes of the chloroplast, termed TOC and TIC, respectively.^{9–13} Discovery of the chloroplast-localized ubiquitin E3 ligase SUPPRESSOR OF PPI1 LOCUS1 (SP1) demonstrated that the nucleocytoplasmic ubiquitin-proteasome system (UPS) targets the TOC apparatus to dynamically control protein import and chloroplast biogenesis in response to developmental and environmental cues. The relevant UPS pathway is termed chloroplast-associated protein degradation (CHLORAD).^{14–16} Two homologs of SP1 exist, SP1-like1 (SPL1) and SPL2, but their roles have remained obscure. Here, we show that SP1 is ubiquitous in the Viridiplantae and that SPL2 and SPL1 appeared early during the evolution of the Viridiplantae and land plants, respectively. Through genetic and biochemical analysis, we reveal that SPL1 functions as a negative regulator of SP1, potentially by interfering with its ability to catalyze ubiquitination. In contrast, SPL2, the more distantly related SP1 homolog, displays partial functional redundancy with SP1. Both SPL1 and SPL2 modify the extent of leaf senescence, like SP1, but do so in diametrically opposite ways. Thus, SPL1 and SPL2 are bona fide CHLORAD system components with negative and positive regulatory functions that allow for nuanced control of this vital proteolytic pathway.

RESULTS

The *SPL2* gene is partially redundant with *SP1*

The *SP1* gene (TAIR: At1g63900) was identified in a genetic screen for second-site suppressors of the *Arabidopsis thaliana* Toc33 knockout mutation, *plastid protein import1* (*ppi1*).¹⁴ The *sp1* mutation causes recovery of the chlorotic *ppi1* phenotype by improving TOC protein stability and, consequently, chloroplast preprotein import capacity and development due to disruption of the CHLORAD proteolytic pathway.¹⁶ Although *SPL1* (TAIR: At1g59560) and *SPL2* (TAIR: At1g54150) share amino acid sequence identity (60.3% and 20.5%, respectively) and topological similarity with *SP1*,¹⁴ their functions are poorly defined. Notwithstanding some alternative reports,^{17–20} confocal microscopy revealed chloroplast envelope localization similar to *SP1* for both homologs.^{14,21} However, *SPL1* overexpression did not

complement the phenotype of *sp1 ppi1* mutants, indicating that *SPL1* is not redundant with *SP1*.¹⁴ Little is known about the role of *SPL2*, although its indirect involvement in drought tolerance via noncoding RNA and an adjacent drought-stress inducible transcription factor gene has been suggested.¹⁷ Given the lack of information concerning the functions of the *SPL* genes, we investigated the possibility that they are regulators of chloroplast biogenesis.

We began by exploring the evolutionary relationship between *SP1* and its homologs. Phylogenetic analysis showed that *SP1* orthologs are ubiquitous across the plant kingdom, including Chlorophyta (green algae) (Figure 1A). Branch lengths for vascular plant species in this group were notably short, indicating very low frequencies of amino acid substitution. This supports the view of *SP1* as an important, highly conserved E3 ligase required for TOC regulation during the biogenesis and operation



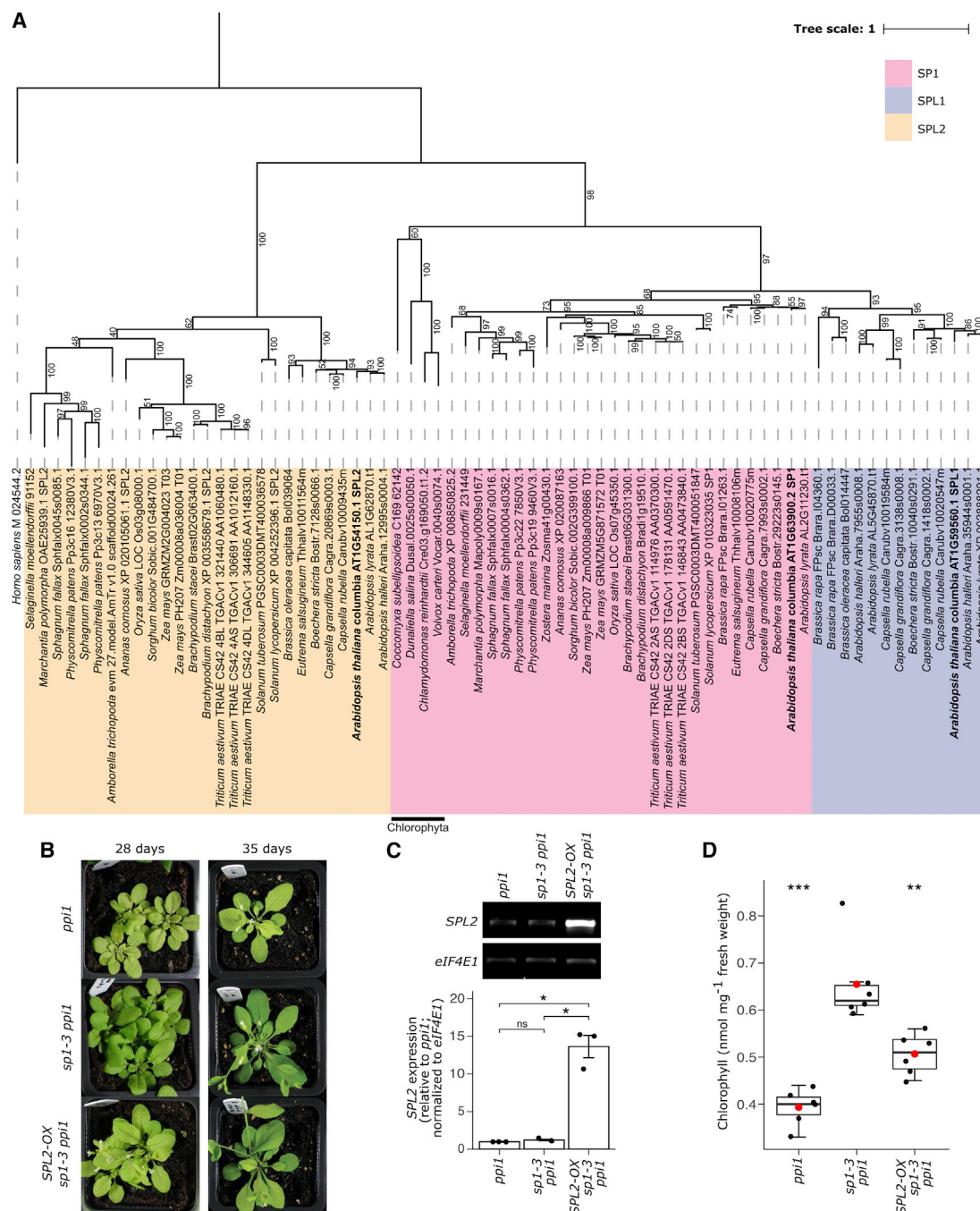


Figure 1. Analysis of the relationship between SP1, SPL1, and SPL2

(A) Phylogenetic analysis of SP1 and its homologs. A bootstrapped maximum likelihood evolutionary analysis of SP1 homologs in the Viridiplantae. Multiple sequence alignment of amino acid sequences retrieved from multiple databases was performed using MergeAlign and the tree was inferred using W-IQ-TREE with 1,000 ultrafast bootstrap replicates. The related human mitochondrial protein MULAN was included as an outgroup. The scale bar indicates the average number of substitutions per site, and percentage ultrafast bootstrap values are shown. The SP1, SPL1, and SPL2 clades are shaded pink, violet, and yellow, respectively. *Arabidopsis thaliana* genes are highlighted in bold text.

(B–D) Analysis of the effects of *SPL2* overexpression (OX) in the *sp1 pp1* double-mutant background. The *Arabidopsis SPL2* cDNA was cloned downstream of the constitutive cauliflower mosaic virus (CaMV) 35S promoter in the binary vector pB2GW7, and corresponding transgenic plants were grown on soil under standard growth conditions for 28 or 35 days before photography (B). Overexpression was confirmed by semi-quantitative RT-PCR analysis of the *SPL2-OX sp1-3 pp1* and control plants using gene-specific primers for *SPL2* and the reference gene *eIF4E1*. The data are shown as mean \pm SEM from three independent experiments (C). Plant chlorophyll contents were measured using a Konica Minolta SPAD-502 meter; data were converted to chlorophyll values as nmol per mg fresh weight (D). Measurements were made from six different individuals and presented as boxplots with the central box representing values between the first and third quartiles and the middle line representing the median value. The whiskers extend to the minimum and maximum values. The red circles indicate the means. The

(legend continued on next page)

of plastids.^{14,15} Furthermore, the close relationship between SP1 and SPL1 was confirmed, as these sequences were derived from a common ancestor within the SP1 clade, right after the divergence of the Embryophyta (land plants) from the Chlorophyta. However, the number of species represented in the SPL1 subclade was greatly reduced, with only members of the Brassicaceae family of flowering plants (including the crops *Brassica oleracea* and *B. rapa*) present. This suggests that SPL1 was subsequently lost in species outside of the Brassicaceae. Branch lengths in the SPL1 subclade were longer than those in the SP1 subclade, revealing accelerated divergence of SPL1 sequences. This may indicate neofunctionalization or pseudogene formation,²² consistent with the non-redundancy conclusion of the earlier complementation experiment.¹⁴

Orthologs of SPL2 were also ubiquitous in land plants (Figure 1A). However, unlike SP1, SPL2 was not present in any of the representative green algal species, so the liverwort *Marchantia polymorpha* was the earliest diverging species with this sequence in our analysis. The SPL2 orthologs formed a monophyletic group that was derived from a common ancestor, which also gave rise to the SP1/SPL1 clade, so we infer that SPL2 was subsequently lost in green algae. Branch lengths in the SPL2 clade were more varied than those in the SP1 clade, implying different SPL2 evolution rates. This suggests greater conservation in some species and more divergence in others.

Potential SPL2 involvement in regulating the chloroplast protein import machinery, suggested by the phylogeny, was investigated by gene complementation in *Arabidopsis*. An SPL2 overexpression (SPL2-OX) construct was stably transformed into *sp1-3 ppi1* plants (Figures 1B and S1A), producing an ~14-fold increase in SPL2 mRNA (Figure 1C). The transgenic plants were visibly paler than *sp1-3 ppi1* controls, with reduced chlorophyll content (Figures 1B, 1D, and S1A). Moreover, the transgenics contained reduced TOC protein levels, relative to *sp1-3 ppi1* control plants, indicating that SPL2 shares functional redundancy with SP1 (Figure S1B). The detected complementation was incomplete, however, as the SPL2-OX *sp1-3 ppi1* plants were still greener than *ppi1* (Figures 1B, 1D, and S1A), suggesting that the redundancy is partial.

The SPL2 gene regulates the chloroplast protein import machinery

Next, the involvement of SPL1 and SPL2 in chloroplast biogenesis was investigated genetically.²³ To do this, we obtained T-DNA knockout mutants for SPL1^{20,24} (Figure S1C), and because suitable T-DNA lines were not available for SPL2,¹⁷ we generated SPL2 knockdown (SPL2-KD) lines using an artificial microRNA (amiRNA) approach.^{25,26} The SPL2-KD construct was stably introduced into wild-type *Arabidopsis*, and a line showing ~20% of the native mRNA level was selected for analysis (Figure S1D). Similar to *sp1* plants,¹⁴ both *sp1* and SPL2-KD plants were visibly indistinguishable from wild type under standard growth conditions (Figure S1E).

The *sp1-1* and SPL2-KD lines were each then crossed to *ppi1* to generate the *sp1-1 ppi1* and SPL2-KD *ppi1* #1 double

mutants (Figure 2A). In parallel, a second SPL2-KD line (termed SPL2-KD *ppi1* #2) was generated by direct transformation into *ppi1* (Figure 2A), and in both lines, SPL2 expression was reduced to ~25% of the native level (Figure 2B).

The *sp1-1 ppi1* double mutants did not display visible or chlorophyll content differences from *ppi1* control plants (Figures 2A and 2C), and this observation was confirmed using a different allele, *sp1-2* (Figures S1F and S1G). In contrast, appreciable recovery of the chlorotic *ppi1* phenotype was apparent in both SPL2-KD *ppi1* lines (Figure 2A), and this was reflected in chlorophyll content measurements (Figure 2C). Moreover, the phenotypic recovery was linked to improved chloroplast development: the chloroplasts in SPL2-KD *ppi1* were larger and more developed than those in *ppi1* (Figures 2D and 2E). In contrast, chloroplasts in *sp1-1 ppi1* were indistinguishable from those in *ppi1* (Figures 2D and 2E).

To understand the molecular basis of the chloroplast developmental recovery in SPL2-KD *ppi1*, chloroplast protein import assays were conducted. Chloroplasts isolated from SPL2-KD *ppi1* and control plants were incubated independently with radiolabeled Rubisco small subunit preprotein, and protein uptake was monitored. Chloroplast protein import in SPL2-KD *ppi1* was improved relative to that in *ppi1* (Figure 3A). This recovery in import capacity was linked to stabilization of the TOC apparatus, as SPL2-KD *ppi1* plants displayed elevated abundance of the Toc75 channel (Figure 3B). That the recovery in Toc75 levels in SPL2-KD *ppi1* was quantitatively smaller than that in *sp1 ppi1* plants (which are null for SP1) was perhaps because SPL2 gene silencing was incomplete (Figure 2B). This might also explain the absence of a significant recovery in the abundance of the receptor, Toc159, which even in *sp1 ppi1* showed only modest recovery.¹⁴

To investigate the possibility that TOC proteins are regulated directly by SPL2 (as they are by SP1), immunoprecipitation (IP) analysis employing YFP-tagged SPL2 (and SP1) was conducted. All the core TOC components (Toc159, Toc75, and Toc33) were detected in fractions that co-eluted with either SPL2-YFP or SP1-YFP but not in control elutions (Figure 3C), and the specificity of the interactions was demonstrated by the absence of non-TOC components (Tic110 and Stic1/Alb4) in the elutions. Thus, we concluded that SPL2 may regulate TOC proteins directly.

SPL1 lacks E3 ligase activity in vitro

Our genetic analyses revealed no suppression of the *ppi1* phenotype in *sp1 ppi1* plants (Figures 2 and 3B). This lack of suppression was not linked to an obvious defect in the E3-defining RING domain of SPL1: RING sequence alignment analysis revealed no obvious differences between SP1 and SPL1 (Figure S2A), and structural models of the cytosolic domains of SP1, SPL1, and SPL2 were similar (Figure S2B). These observations prompted us to investigate whether SPL1 and SPL2 possess E3 ligase activity, similar to SP1, by conducting *in vitro* auto-ubiquitination assays.¹⁴

Polyubiquitin smears (indicating catalytic activity) were observed for both SP1 and SPL2 (Figures 4A and S2C–S2E), indicating that SPL2 is an active E3 ligase. These smears were absent

black circles in (C) and (D) show the individual data points. The p values were derived from Student's t test analysis (two-tailed) of the means of the indicated genotypes (ns, not significant; *p < 0.05; **p < 0.01; ***p < 0.001). The *sp1-3 ppi1* genotype was used as the reference group for the statistical analysis in (D). See also Figure S1.

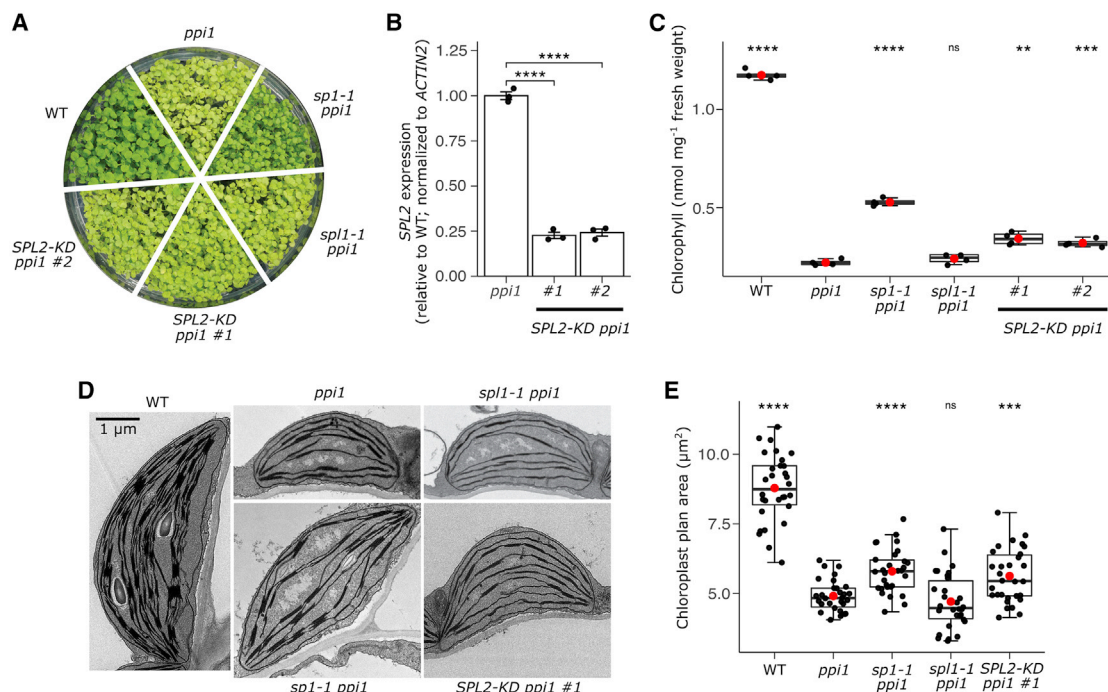


Figure 2. Inactivation of *SPL2*, but not *SPL1*, results in suppression of the *ppi1* phenotype

(A) Visible appearance of the different plant genotypes. Wild-type, *ppi1*, *sp1-1 ppi1*, *sp1-1 ppi1*, *SPL2-KD ppi1* #1, and *SPL2-KD ppi1* #2 plants were grown on MS medium under standard growth conditions for 2 weeks before photography.

(B) Assessment of *SPL2* expression in the knockdown lines by qRT-PCR. The analysis was performed using gene-specific primers for *SPL2* and the reference gene *ACTIN2*. The data are shown as mean \pm SEM from three independent experiments.

(C) Chlorophyll content analysis of the different genotypes. Chlorophyll was measured photometrically following DMF extraction from 10-day-old seedlings grown *in vitro*. Extraction was from 10 seedlings per genotype for each measurement. A total of four independent experiments were performed for each genotype, and the data were presented as boxplots (see below for details).

(D and E) Transmission electron microscopy analysis of chloroplast development. Rosette leaf tissue from 35-day-old plants grown on soil under standard growth conditions was fixed and analyzed. Representative micrographs showing typical chloroplasts from each genotype are shown (D). Scale bar indicates 1 μ m. Micrographs similar to those in (D) of 30 chloroplasts per genotype were quantitatively analyzed, and the calculated organelle plan area data were presented as boxplots (E).

In (C) and (E), the central box represents values between the first and the third quartiles, and the middle line represents the median value. The whiskers extend to the minimum and maximum values. The red circles indicate the means. The black circles in (B), (C), and (E) show the individual data points. For (B), (C), and (E), the *p* values were derived from Student's *t* test analysis (two-tailed) of the means of the indicated genotypes (ns, not significant; ***p* < 0.01; ****p* < 0.001; *****p* < 0.0001). The *ppi1* genotype was used as the reference group for the statistical analysis.

See also Figure S1.

in reactions containing the corresponding RING mutants (C330A and H348Y, respectively), confirming the specificity of the results and the importance of the mutated residues for functionality. However, no ubiquitination activity was detected for *SPL1* or its RING mutant (H308Y), using two different E2 enzymes (Figures 4A and S2C–S2E). This implies that *SPL1* does not possess similar E3 activity to *SP1* and *SPL2*, which may indicate that *SPL1* is a non-functional enzyme; alternatively, *SPL1* may require an E2 different from those tested, be subject to autoinhibition that cannot be overcome *in vitro*, have distinct substrate requirements, or be unable to catalyze formation of polyubiquitin chains.

***SPL1* and *SPL2* are both important during leaf senescence**

Plastid transition processes (such as those occurring during leaf senescence) are delayed in *sp1* mutants and promoted in *SP1* overexpressor (*SP1-OX*) plants.¹⁴ To assess whether the *SPL2-SP1* redundancy extends to such transitions, we analyzed

the effect of *SPL2* (and, for comparison, *SP1* and *SPL1*) on senescence induction by dark treatment.

Before dark treatment, all genotypes were phenotypically similar to the wild type (Figures S3A and S3B), but upon senescence induction, clear differences became apparent (Figure 4B). Effects of *SPL2* manipulation resembled closely those of *SP1* manipulation: *SPL2-KD* exhibited delayed senescence, whereas *SPL2-OX* exhibited enhanced senescence, and these effects were quantified by measuring chlorophyll content (Figure 4C) and photosynthetic efficiency (Figure S3C). A different, unanticipated effect was observed in *sp1-1*: senescence was accelerated, closely resembling the effect of *SP1-OX* (Figures 4B, 4C, and S3C). This phenomenon was consistent across different *sp1* alleles (Figure S3D). Furthermore, *sp1-1 sp1-1* leaves also showed rapid senescence (Figures 4B, 4C, and S3C), indicating that *sp1* was epistatic over *sp1* in this regard.

In accordance with the notion that *SP1* and *SPL1* exert opposing effects on plant development (an idea also suggested

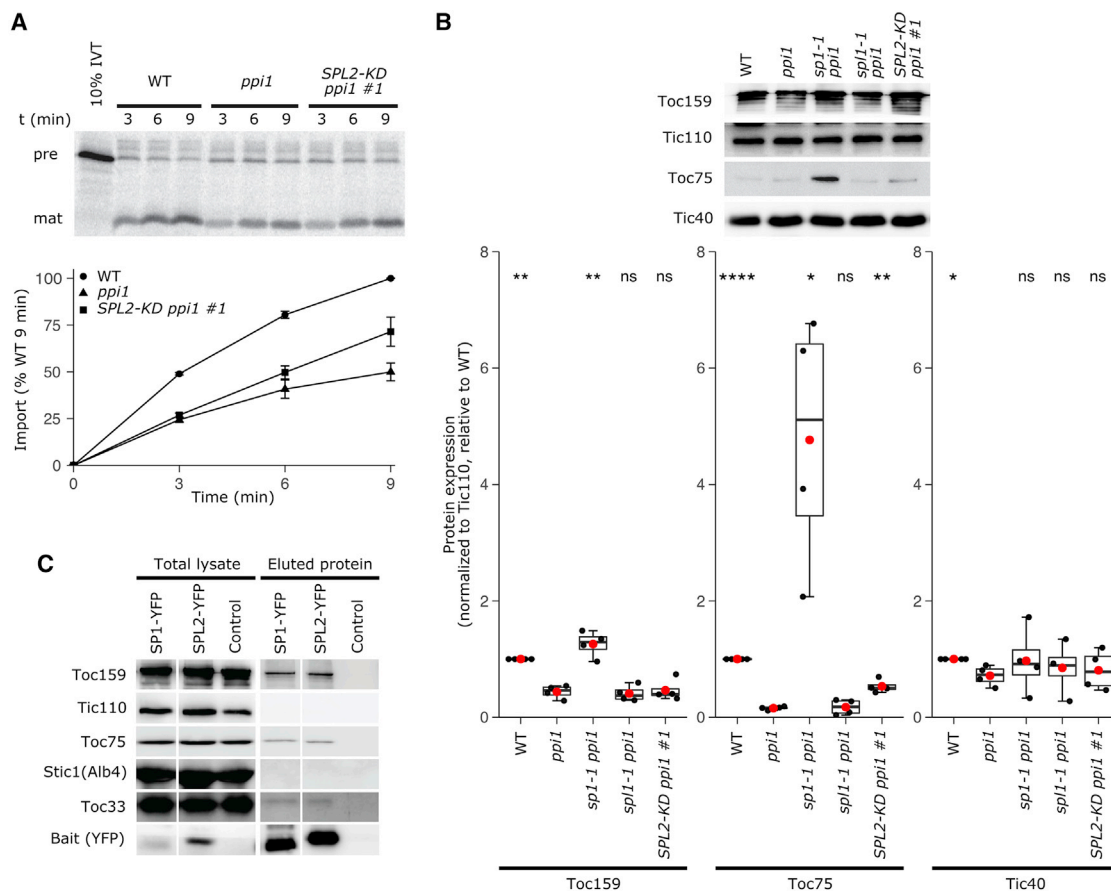


Figure 3. Suppression mediated by *SPL2* knockdown is linked to the chloroplast protein import machinery

(A) *In vitro* chloroplast protein import assays. Chloroplasts isolated from 14-day-old wild-type, *ppl1*, and *SPL2-KD ppl1 #1* plants were incubated with *in vitro* translated (IVT) Rubisco small subunit preprotein (pre) and processing to the mature (mat) form was assessed over a time course (3, 6, and 9 min). The amount of mature imported protein at each time point was quantified and expressed as a percentage of the amount of protein imported into wild-type chloroplasts at 9 min. The data shown are means \pm SEM from three independent experiments.

(B) Immunoblot analysis of TOC protein accumulation. Total protein samples extracted from 2-week-old seedlings of the indicated genotypes were analyzed by immunoblotting using different TOC and TIC antibodies. Bands from three independent experiments were quantified, and the data are shown as boxplots. The central box represents values between the first and third quartiles, and the middle line represents the median value. The whiskers extend to the minimum and maximum values. The red circles indicate the means, and the black circles show the individual data points. The *ppl1* genotype was used as the reference group for the statistical analysis.

(C) Immunoprecipitation analyses of physical interactions with TOC proteins. The SP1 and SPL2 proteins were transiently expressed as YFP fusions in *Arabidopsis* protoplasts, and employed as immunoprecipitation baits. The SP1-YFP fusion was included as a positive control for TOC interaction, whereas a negative control sample lacking a fusion protein was used as a negative control to confirm the specificity of the detected interactions. Protein samples were analyzed by immunoblotting using antibodies against: the YFP tag (anti-GFP was employed), to verify the enrichment of the fusion proteins; TOC components, to assess for substrate interactions; the Tic110 and Stic1/Alb4 proteins, to confirm the specificity of the detected TOC interactions. The low level of SP1-YFP detected in the total lysate sample was as expected, and likely due to the autoregulatory properties of the SP1 protein.¹⁴

in a previous study, in a different context²⁰), whereas the expression of *SP1* increased during senescence, that of *SPL1* decreased markedly in senescent tissues (Figure S3E).²⁷ In contrast, *SPL2* expression remained largely unchanged.

SPL1* negatively regulates the E3 ligase activity of *SP1

Based on the results discussed above, we hypothesized that *SPL1* inhibits the activity of *SP1* via an unknown mechanism. To test this hypothesis, we performed *in vitro* auto-ubiquitination assays similar to those described earlier, except here the E3 proteins were mixed together in different ratios. In agreement with

our hypothesis, a reducing trend of ubiquitination was observed when *SPL1* was added in excess of *SP1* (Figure 4D). A control experiment using mutant *SP1* (C330A) in place of *SPL1* did not yield a similar effect on *SP1* activity (Figure 4D). Although it is possible that *SPL1* inhibited activity in this context by titrating E2 enzyme in a way that the *SP1* RING mutant could not, this result implied that *SPL1* functions as an inhibitor of *SP1* activity. In support of this idea, coIP demonstrated physical interaction of *SPL1* with *SP1* *in vivo* (Figure S4A).

Next, the phenotypic consequences of overexpressing *SP1* and *SPL1* in the *ppl1* background, either in isolation or in

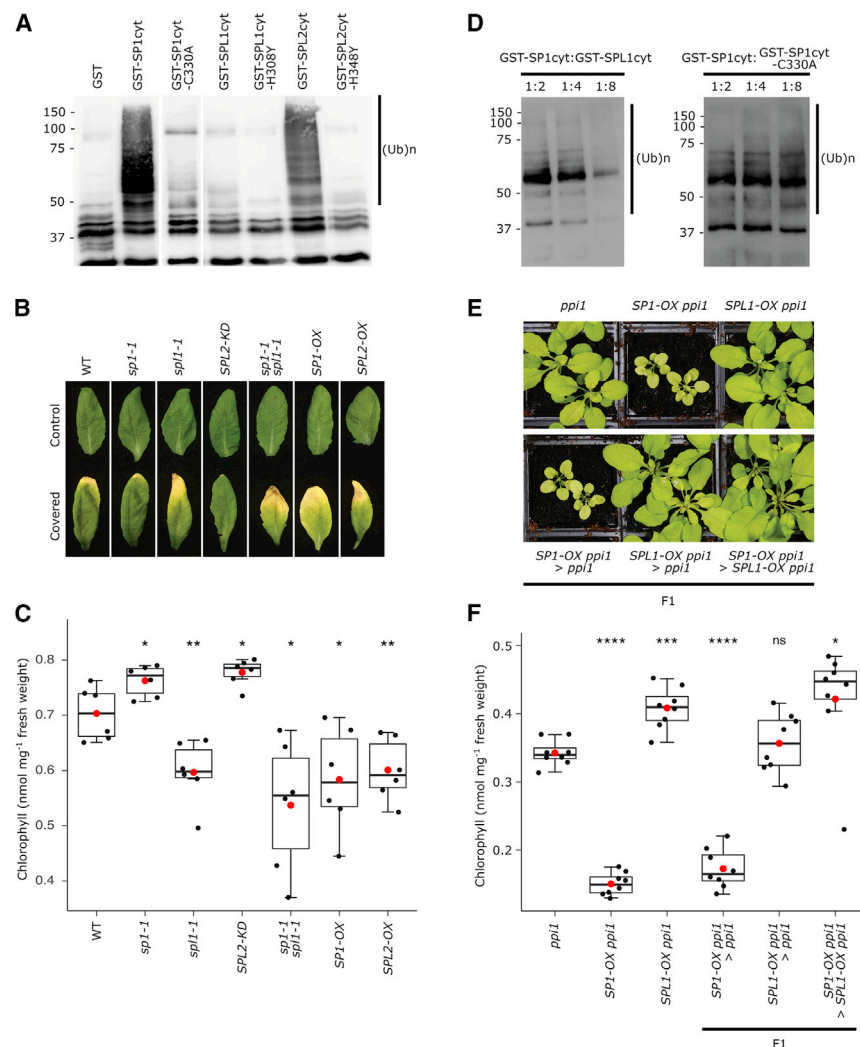


Figure 4. SPL1 lacks E3 ligase activity but acts in opposition to SP1 and SPL2

(A) *In vitro* auto-ubiquitination analysis of SP1 and SPL1. Bacterially expressed GST and GST fusions of the indicated SP1/SPL cytosolic domains (cyt; this domain was previously shown to be the minimal requirement for activity with SP1)¹⁴ were incubated in a standard reaction containing all other components required for ubiquitination (human E1, 6×His-tagged AtUBC8 E2, and HA-tagged ubiquitin). A mutant version of each protein was included as a negative control; these mutants were generated by substituting a conserved residue in the C3HC4 RING domain.^{14,17} The reaction products were resolved by immunoblotting using anti-HA antibody, to detect ubiquitinated species. Ubiquitination activity was indicated by the presence of high molecular weight bands of varying sizes, as indicated by the bar labeled (Ub)_n.

(B and C) Analysis of effects on leaf senescence. Rosette leaves of 28-day-old plants were induced to senesce by covering with aluminum foil for 5 days. The leaves were excised at the end of the dark treatment and photographed (B); control leaves were left uncovered. Chlorophyll contents of the indicated genotypes were measured using a Konica Minolta SPAD-502 meter; data were converted to chlorophyll values as nmol per mg fresh weight (C). The data were derived from six different individuals and are presented as boxplots (see below for details).

(D) Analysis of the inhibitory effect of SPL1 on SP1 auto-ubiquitination activity *in vitro*. Bacterially expressed GST-tagged proteins as described in (A) were mixed in different ratios with GST-SP1cyt, as indicated, and then the mixtures were employed in standard ubiquitination reactions as before. Reaction products were analyzed by immunoblotting as in (A).

(E and F) Analysis of the effects of combined overexpression of SP1 and SPL1. Visible appearance of plants carrying different combinations of the *SP1-OX* and *SPL1-OX* transgenes in the *ppi1*

mutant background. Plants shown in the lower panel are the F1 progeny of the indicated crosses. Plants were grown on soil under standard growth conditions for 28 days before photography (E). Chlorophyll contents of the indicated genotypes were measured using a Konica Minolta SPAD-502 meter; data were converted to chlorophyll values as nmol per mg fresh weight (F). Measurements were recorded from eight different individuals and presented as boxplots.

In (C) and (F), the central box represents values between the first and third quartiles, and the middle line represents the median value. The whiskers extend to the minimum and maximum values. The red circles indicate the means, and the black circles show the individual data points. The p values were derived from Student's t test analysis (two-tailed) of the means of the indicated genotypes (ns, not significant; *p < 0.05; **p < 0.01; ***p < 0.001; ****p < 0.0001). The *ppi1* genotype was used as the reference group for the statistical analysis.

See also Figures S2–S4.

combination, were assessed (Figures 4E, 4F, and S4B). The *SP1-OX ppi1* plants were very small and had lower chlorophyll and TOC protein levels than *ppi1*, as expected.¹⁴ In contrast, *SPL1-OX ppi1* plants were slightly greener than *ppi1* and had similar TOC protein levels. Most significantly, double overexpressors of *SP1* and *SPL1* in the *ppi1* background closely resembled *SPL1-OX ppi1* plants in relation to chlorophyll content and TOC abundance. Thus, *SPL1* overexpression abrogates the effects of *SP1* overexpression, which aligns with the *in vitro* data (Figure 4D) and supports the hypothesis that *SPL1* negatively regulates *SP1* activity. Because *SPL1* physically interacts with TOC proteins (Figure S4C), in addition to *SP1* (Figure S4A), it appears that *SPL1* and *SP1* both interact with TOC complexes, potentially acting in competition with each other.

DISCUSSION

The requirement for the TOC-TIC machinery to import >90% of chloroplast proteins is well known,^{2,28} but the regulation of such import was until recently not well understood. The discovery of SP1 and CHLORAD set a new paradigm by establishing post-translational control of the TOC apparatus by the UPS as a crucial regulatory circuit.^{14,16}

SPL1 is a negative regulator of SP1

The SPL1 and SPL2 proteins were identified as homologs of SP1,¹⁴ but reliable information on their evolutionary relationships has been lacking.^{24,29} Here, SP1 and SPL2 were each observed to form a discrete monophyletic group, with SPL1 arising from a

duplication event within the SP1 clade (Figure 1A). Elongated SPL1 branch lengths, together with the observation that *SPL1* cannot complement *sp1*,¹⁴ led us to hypothesize that SPL1 has acquired a function distinct from that of SP1.

Though it possesses an apparently normal RING domain (Figures S2A and S2B), SPL1 lacks E3 activity *in vitro* (Figures 4A and S2E). One possible explanation is that *SPL1* is a pseudogene, as it shares a similar gene structure with its paralogue, *SP1*.^{14,30} However, this is unlikely because the *SPL1* open reading frame is just five codons shorter than that of *SP1* and *SPL1* expression is robust (Figure S3E). Moreover, clear evidence that SPL1 is functional was provided by the accelerated leaf senescence of *sp1* mutants (Figures 4B, 4C, S3C, and S3D), indicating that SPL1 is important for plastid function and plant development.

The possibility that SPL1 negatively influences SP1 activity was suggested by the opposing *SP1* and *SPL1* expression patterns during leaf senescence (Figure S3E), supported by *in vitro* ubiquitination (Figure 4D) and colP assays (Figure S4A), and confirmed by analyses of plants overexpressing both *SP1* and *SPL1* (Figures 4E, 4F, and S4B). How SPL1 inhibits SP1 activity is uncertain, but one possibility is that it functions as a dominant-negative protein by competing with SP1 for binding to either substrate proteins or UPS components or by binding to SP1 itself. That SPL1 may act in opposition to SP1 was also suggested by peroxisomal β -oxidation measurements and effects on the physiology and growth of peroxisomal mutants, although E3 activity of SPL1 was not directly assessed.²⁰ Most likely, these effects were indirect consequences of SPL1's inhibitory role in CHLORAD, owing to the close functional links between chloroplasts and peroxisomes.³¹

The emergence of SPL1 as a negative regulator of CHLORAD raised interesting questions concerning the evolutionary events following the founding *SP1/SPL1* duplication event. One possibility is that SPL1 is a functional pseudogenic protein that interferes with the product of the parental gene.^{32,33} A more likely circumstance is that *SPL1* arose from *SP1* by a process of neofunctionalization.²² Why is *SPL1* now restricted to the Brassicaceae, having been lost in other land plant families? The Brassicaceae are recognized as the highest speciation group of land plants,³⁴ which may be significant; perhaps the nuanced control of CHLORAD that SPL1 provides is particularly advantageous in these species. It is possible that other species lack this level of control or that proteins other than SPL1 provide regulation. Another possibility is that SP1 in these species has evolved a self-regulation mechanism involving an unidentified SP1 domain; this might explain why the branch lengths outside of the Brassicaceae in the SP1 clade are longer (Figure 1A).

SPL2 shares incomplete functional redundancy with SP1

Similar to SP1, SPL2 is a chloroplast-localized ubiquitin E3 ligase that selectively targets TOC components to control protein import (Figures 1, 2, and 3). That the *ppi1* suppression delivered by *SPL2-KD* was weaker than that of *sp1* was likely due in part to residual *SPL2* gene expression. However, this also suggests that SP1 is the dominant regulator of the TOC machinery and that the *SP1* gene compensates effectively in the *SPL2-KD* line—a notion consistent with the fact that *SP1*, but not *SPL2*, was identified in the original *ppi1* suppressor screen.¹⁴

The consequences of *SPL2* expression manipulation for leaf senescence closely mimic those of *SP1* manipulation, revealing an important role for SPL2 in plastid operation and plant development (Figures 4B, 4C, and S3C). In fact, a recent study showed that this role also involves regulation of chromoplast formation during tomato fruit ripening.³⁵ It is noteworthy that both SP1 and SPL2 have been implicated in abiotic stress responses: SP1 promotes tolerance of salt, osmotic, and oxidative stresses by reducing chloroplast protein import to limit photosynthesis and overaccumulation of damaging reactive oxygen species,¹⁵ whereas *SPL2/NERF* was proposed to promote drought tolerance, albeit via a different mechanism.¹⁷ Differential regulation by two different E3 ligases may enable greater control in response to diverse abiotic stresses.

Regulation of substrates by multiple E3 ligases has been well documented in other systems.^{36,37} With regard to TOC regulation, whether SP1 and SPL2 function independently or cooperatively is uncertain. What is clear, though, is that the functions of SP1 and SPL2 do not completely overlap. Thus, SPL2 may act on additional chloroplast substrates that are not regulated by SP1 (which is strongly focused on TOC regulation). The existence of multiple chloroplast E3 ligases with distinct substrate ranges supports the view that the UPS has an even greater role in chloroplast biology than was previously envisaged and that the scope of CHLORAD is not limited to protein import control.³⁸

STAR★METHODS

Detailed methods are provided in the online version of this paper and include the following:

- KEY RESOURCES TABLE
- RESOURCE AVAILABILITY
 - Lead contact
 - Materials availability
 - Data and code availability
- EXPERIMENTAL MODEL AND SUBJECT DETAILS
- METHOD DETAILS
 - Physiological analysis
 - Generation of transgenic plant lines
 - Characterization of mutant and transgenic plant lines
 - Immunoprecipitation
 - Phylogenetic analysis
 - Protein structural modelling
 - Transmission electron microscopy
 - Recombinant proteins and *in vitro* ubiquitination assays
- QUANTIFICATION AND STATISTICAL ANALYSIS

SUPPLEMENTAL INFORMATION

Supplemental information can be found online at <https://doi.org/10.1016/j.cub.2023.01.060>.

ACKNOWLEDGMENTS

We are grateful to Weihua Huang and Will Broad for early preparatory work on the mutant plant lines, to Naresh Loudya for technical assistance, and to Jane Langdale for guidance and valuable discussions concerning the phylogenetic

analysis. This work was supported by a Brunei Government Ministry of Education Scholarship (to S.M.A.) and by the UK Research and Innovation Biotechnology and Biological Sciences Research Council (UKRI-BBSRC to R.P.J.). This research was funded in whole or in part by UKRI (BB/H008039/1, BB/K018442/1, BB/N006372/1, BB/R009333/1, BB/R016984/1, and BB/V007300/1). For the purpose of Open Access, the author has applied a CC BY public copyright licence to any Author Accepted Manuscript (AAM) version arising from this submission.

AUTHOR CONTRIBUTIONS

S.M.A. designed and conducted the experiments, analyzed the data, and wrote the manuscript; N.L. performed the immunoprecipitation experiments; Z.S. assisted with the transgenic analyses and the immunoblot experiments; E.J. prepared the TEM samples and S.M.A. performed the corresponding imaging and analysis; Q.L. and S.M.A. generated the constructs and transgenic plants; J.Y. assisted with the *in vitro* auto-ubiquitination assays; and R.P.J. conceived of the study, supervised the work, analyzed the data, and wrote the manuscript.

DECLARATION OF INTERESTS

The application of CHLORAD as a technology for crop improvement is covered by a patent application (no. WO2019/171091 A).

Received: March 30, 2021

Revised: December 2, 2022

Accepted: January 26, 2023

Published: February 22, 2023

REFERENCES

- Whatley, J.M. (1978). A suggested cycle of plastid developmental interrelationships. *New Phytol.* **80**, 489–502.
- Jarvis, P., and López-Juez, E. (2013). Biogenesis and homeostasis of chloroplasts and other plastids. *Nat. Rev. Mol. Cell Biol.* **14**, 787–802.
- Sadali, N.M., Sowden, R.G., Ling, Q., and Jarvis, R.P. (2019). Differentiation of chloroplasts and other plastids in plants. *Plant Cell Rep.* **38**, 803–818.
- Bruce, B.D. (2000). Chloroplast transit peptides: structure, function and evolution. *Trends Cell Biol.* **10**, 440–447.
- Lee, D.W., and Hwang, I. (2018). Evolution and design principles of the diverse chloroplast transit peptides. *Mol. Cells* **41**, 161–167.
- Jarvis, P. (2008). Targeting of nucleus-encoded proteins to chloroplasts in plants. *New Phytol.* **179**, 257–285.
- Schnell, D.J. (2019). The TOC GTPase receptors: regulators of the fidelity, specificity and substrate profiles of the general protein import machinery of chloroplasts. *Protein J.* **38**, 343–350.
- Demarsy, E., Lakshmanan, A.M., and Kessler, F. (2014). Border control: selectivity of chloroplast protein import and regulation at the TOC-complex. *Front. Plant Sci.* **5**, 483.
- Li, H.M., and Chiu, C.C. (2010). Protein transport into chloroplasts. *Annu. Rev. Plant Biol.* **61**, 157–180.
- Richardson, L.G.L., Singhal, R., and Schnell, D.J. (2017). The integration of chloroplast protein targeting with plant developmental and stress responses. *BMC Biol.* **15**, 118.
- Shi, L.-X., and Theg, S.M. (2013). The chloroplast protein import system: from algae to trees. *Biochim. Biophys. Acta.* **1833**, 314–331.
- Li, H.M., Schnell, D., and Theg, S.M. (2020). Protein import motors in chloroplasts: on the role of chaperones. *Plant Cell* **32**, 536–542.
- Nakai, M. (2020). Reply: The revised model for chloroplast protein import. *Plant Cell* **32**, 543–546.
- Ling, Q., Huang, W., Baldwin, A., and Jarvis, P. (2012). Chloroplast biogenesis is regulated by direct action of the ubiquitin-proteasome system. *Science* **338**, 655–659.
- Ling, Q., and Jarvis, P. (2015). Regulation of chloroplast protein import by the ubiquitin E3 ligase SP1 is important for stress tolerance in plants. *Curr. Biol.* **25**, 2527–2534.
- Ling, Q., Broad, W., Trösch, R., Töpel, M., Demiral Sert, T.D., Lymperopoulos, P., Baldwin, A., and Jarvis, R.P. (2019). Ubiquitin-dependent chloroplast-associated protein degradation in plants. *Science* **363**, eaav4467.
- Gao, W., Liu, W., Zhao, M., and Li, W.X. (2015). NERF encodes a RING E3 ligase important for drought resistance and enhances the expression of its antisense gene NFYA5 in Arabidopsis. *Nucleic Acids Res.* **43**, 607–617.
- Pan, R., Satkovich, J., and Hu, J. (2016). E3 ubiquitin ligase SP1 regulates peroxisome biogenesis in Arabidopsis. *Proc. Natl. Acad. Sci. USA* **113**, E7307–E7316.
- Pan, R., and Hu, J. (2018). The Arabidopsis E3 ubiquitin ligase SP1 targets to chloroplasts, peroxisomes, and mitochondria. *Plant Physiol.* **176**, 480–482.
- Pan, R., Satkovich, J., Chen, C., and Hu, J. (2018). The E3 ubiquitin ligase SP1-like 1 plays a positive role in peroxisome biogenesis in Arabidopsis. *Plant J.* **94**, 836–846.
- Ling, Q., Li, N., and Jarvis, P. (2017). Chloroplast ubiquitin E3 ligase SP1: does it really function in peroxisomes? *Plant Physiol.* **175**, 586–588.
- Xiao, J., Sekhwal, M.K., Li, P., Ragupathy, R., Cloutier, S., Wang, X., and You, F.M. (2016). Pseudogenes and their genome-wide prediction in plants. *Int. J. Mol. Sci.* **17**.
- Jarvis, P., Chen, L.J., Li, H., Peto, C.A., Fankhauser, C., and Chory, J. (1998). An Arabidopsis mutant defective in the plastid general protein import apparatus. *Science* **282**, 100–103.
- Basnayake, B.M.V.S., Li, D., Zhang, H., Li, G., Virk, N., and Song, F. (2011). Arabidopsis DAL1 and DAL2, two ring finger proteins homologous to Drosophila DIAP1, are involved in regulation of programmed cell death. *Plant Cell Rep.* **30**, 37–48.
- Ossowski, S., Schwab, R., and Weigel, D. (2008). Gene silencing in plants using artificial microRNAs and other small RNAs. *Plant J.* **53**, 674–690.
- Schwab, R., Ossowski, S., Riester, M., Warthmann, N., and Weigel, D. (2006). Highly specific gene silencing by artificial microRNAs in Arabidopsis. *Plant Cell* **18**, 1121–1133.
- Hruz, T., Laule, O., Szabo, G., Wessendorp, F., Bleuler, S., Oertle, L., Widmayer, P., Gruissem, W., and Zimmermann, P. (2008). Genevestigator V3: a reference expression database for the meta-analysis of transcriptomes. *Adv. Bioinformatics* **2008**, 420747.
- Paila, Y.D., Richardson, L.G.L., and Schnell, D.J. (2015). New insights into the mechanism of chloroplast protein import and its integration with protein quality control, organelle biogenesis and development. *J. Mol. Biol.* **427**, 1038–1060.
- Pan, R., and Hu, J. (2017). Sequence and biochemical analysis of Arabidopsis SP1 protein, a regulator of organelle biogenesis. *Commun. Integr. Biol.* **10**, e1338991.
- Tutar, Y. (2012). Pseudogenes. *Comp. Funct. Genomics* **2012**, 424526.
- Albrecht, V., Simková, K., Carrie, C., Delannoy, E., Giraud, E., Whelan, J., Small, I.D., Apel, K., Badger, M.R., and Pogson, B.J. (2010). The cytoskeleton and the peroxisomal-targeted snowy cotyledon3 protein are required for chloroplast development in Arabidopsis. *Plant Cell* **22**, 3423–3438.
- Xiao-Jie, L., Ai-Mei, G., Li-Juan, J., and Jiang, X. (2015). Pseudogene in cancer: real functions and promising signature. *J. Med. Genet.* **52**, 17–24.
- Poliseno, L. (2012). Pseudogenes: newly discovered players in human cancer. *Sci. Signal.* **5**, re5.
- Hohmann, N., Wolf, E.M., Lysak, M.A., and Koch, M.A. (2015). A time-calibrated road map of Brassicaceae species radiation and evolutionary history. *Plant Cell* **27**, 2770–2784.
- Ling, Q., Sadali, N.M., Soufi, Z., Zhou, Y., Huang, B., Zeng, Y., Rodriguez-Concepcion, M., and Jarvis, R.P. (2021). The chloroplast-associated protein degradation pathway controls chloroplast development and fruit ripening in tomato. *Nat. Plants* **7**, 655–666.

36. Lee, J.T., and Gu, W. (2010). The multiple levels of regulation by p53 ubiquitination. *Cell Death Differ.* **17**, 86–92.
37. Kelley, D.R., and Estelle, M. (2012). Ubiquitin-mediated control of plant hormone signaling. *Plant Physiol.* **160**, 47–55.
38. Sun, Y., Yao, Z., Ye, Y., Fang, J., Chen, H., Lyu, Y., Broad, W., Fournier, M., Chen, G., Hu, Y., et al. (2022). Ubiquitin-based pathway acts inside chloroplasts to regulate photosynthesis. *Sci. Adv.* **8**, eabq7352.
39. Trösch, R., Töpel, M., Flores-Pérez, Ú., and Jarvis, P. (2015). Genetic and physical interaction studies reveal functional similarities between ALBINO3 and ALBINO4 in Arabidopsis. *Plant Physiol.* **169**, 1292–1306.
40. Aronsson, H., Combe, J., Patel, R., Agne, B., Martin, M., Kessler, F., and Jarvis, P. (2010). Nucleotide binding and dimerization at the chloroplast pre-protein import receptor, atToc33, are not essential in vivo but do increase import efficiency. *Plant J.* **63**, 297–311.
41. Kasmati, A.R., Töpel, M., Patel, R., Murtaza, G., and Jarvis, P. (2011). Molecular and genetic analyses of Tic20 homologues in Arabidopsis thaliana chloroplasts. *Plant J.* **66**, 877–889.
42. Bauer, J., Chen, K., Hiltbunner, A., Wehrli, E., Eugster, M., Schnell, D., and Kessler, F. (2000). The major protein import receptor of plastids is essential for chloroplast biogenesis. *Nature* **403**, 203–207.
43. Aronsson, H., Combe, J., and Jarvis, P. (2003). Unusual nucleotide-binding properties of the chloroplast protein import receptor, atToc33. *FEBS Lett.* **544**, 79–85.
44. Karimi, M., Inzé, D., and Depicker, A. (2002). GATEWAY vectors for Agrobacterium-mediated plant transformation. *Trends Plant Sci.* **7**, 193–195.
45. Aronsson, H., and Jarvis, R.P. (2011). Rapid isolation of Arabidopsis chloroplasts and their use for in vitro protein import assays. *Methods Mol. Biol.* **774**, 281–305.
46. Collingridge, P.W., and Kelly, S. (2012). MergeAlign: improving multiple sequence alignment performance by dynamic reconstruction of consensus multiple sequence alignments. *BMC Bioinformatics* **13**, 117.
47. Katoh, K., Kuma, K., Toh, H., and Miyata, T. (2005). MAFFT version 5: improvement in accuracy of multiple sequence alignment. *Nucleic Acids Res.* **33**, 511–518.
48. Trifinopoulos, J., Nguyen, L.T., von Haeseler, A., and Minh, B.Q. (2016). W-IQ-TREE: a fast online phylogenetic tool for maximum likelihood analysis. *Nucleic Acids Res.* **44**, W232–W235.
49. Letunic, I., and Bork, P. (2016). Interactive tree of life (iTOL) v3: an online tool for the display and annotation of phylogenetic and other trees. *Nucleic Acids Res.* **44**, W242–W245.
50. Zhang, Y. (2008). I-TASSER server for protein 3D structure prediction. *BMC Bioinformatics* **9**, 40.
51. Roy, A., Kucukural, A., and Zhang, Y. (2010). I-TASSER: a unified platform for automated protein structure and function prediction. *Nat. Protoc.* **5**, 725–738.
52. Schindelin, J., Arganda-Carreras, I., Frise, E., Kaynig, V., Longair, M., Pietzsch, T., Preibisch, S., Rueden, C., Saalfeld, S., Schmid, B., et al. (2012). Fiji: an open-source platform for biological-image analysis. *Nat. Methods* **9**, 676–682.
53. Kovacheva, S., Bédard, J., Patel, R., Dudley, P., Twell, D., Rios, G., Koncz, C., and Jarvis, P. (2005). In vivo studies on the roles of Tic110, Tic40 and Hsp93 during chloroplast protein import. *Plant J.* **41**, 412–428.
54. Ling, Q., Huang, W., and Jarvis, P. (2011). Use of a SPAD-502 meter to measure leaf chlorophyll concentration in Arabidopsis thaliana. *Photosynth. Res.* **107**, 209–214.
55. Clough, S.J., and Bent, A.F. (1998). Floral dip: a simplified method for Agrobacterium-mediated transformation of Arabidopsis thaliana. *Plant J.* **16**, 735–743.
56. Flores-Pérez, Ú., and Jarvis, P. (2017). Isolation and suborganellar fractionation of Arabidopsis chloroplasts. *Methods Mol. Biol.* **1511**, 45–60.
57. Flores-Pérez, Ú., Bédard, J., Tanabe, N., Lymperopoulos, P., Clarke, A.K., and Jarvis, P. (2016). Functional analysis of the Hsp93/ClpC chaperone at the chloroplast envelope. *Plant Physiol.* **170**, 147–162.
58. Wu, F.H., Shen, S.C., Lee, L.Y., Lee, S.H., Chan, M.T., and Lin, C.S. (2009). Tape-Arabidopsis sandwich – a simpler Arabidopsis protoplast isolation method. *Plant Methods* **5**, 16.
59. Goodstein, D.M., Shu, S., Howson, R., Neupane, R., Hayes, R.D., Fazo, J., Mitros, T., Dirks, W., Hellsten, U., Putnam, N., and Rokhsar, D.S. (2012). Phytozome: a comparative platform for green plant genomics. *Nucleic Acids Res.* **40**, D1178–D1186.
60. Zerbino, D.R., Achuthan, P., Akanni, W., Amode, M.R., Barrell, D., Bhai, J., Billis, K., Cummins, C., Gall, A., Girón, C.G., et al. (2018). Ensembl 2018. *Nucleic Acids Res.* **46**, D754–D761.
61. Hyman, S., and Jarvis, R.P. (2011). Studying Arabidopsis chloroplast structural organisation using transmission electron microscopy. *Methods Mol. Biol.* **774**, 113–132.
62. Hussain, H., and Chong, N.F.M. (2016). Combined overlap extension PCR method for improved site directed mutagenesis. *BioMed Res. Int.* **2016**, 8041532.

STAR★METHODS

KEY RESOURCES TABLE

REAGENT or RESOURCE	SOURCE	IDENTIFIER
Antibodies		
anti-atStic1/Alb4	Trösch et al ³⁹	N/A
anti-atTic110	Aronsson et al ⁴⁰	N/A
anti-atTic40	Kasmati et al ⁴¹	N/A
anti-atToc159	Bauer et al ⁴²	N/A
anti-atToc33	Aronsson et al ⁴³	N/A
anti-atToc75-III	Kasmati et al ⁴¹	N/A
anti-H3	Abcam	Cat#ab1791; RRID: AB_302613
anti-GFP	Sigma	Cat#SAB4301138; RRID: AB_2750576
anti-HA tag	Sigma	Cat#H6908; RRID: AB_260070
anti-Myc	Abcam	Cat#ab9106; RRID: AB_307014
anti-rabbit IgG HRP	Sigma	Cat#12-348; RRID: AB_390191
Bacterial and virus strains		
α -Select Silver Competent Cells	Bioline	Cat#BIO-85026
<i>Agrobacterium tumefaciens</i> GV3101 (pMP90)	Karimi et al ⁴⁴	N/A
<i>Escherichia coli</i> Rosetta (DE3) cells	Sigma	Cat#70954
Chemicals, peptides, and recombinant proteins		
precursor of small subunit of Rubisco (pSSU)	Aronsson and Jarvis ⁴⁵	N/A
³⁵ S-methionine	Perkin-Elmer	Cat#NEG072002MC
6xHis-tagged AtUBC8 E2	Ling et al ¹⁴	N/A
human UbcH5b	Boston Biochem	Cat#E2-622
bortezomib	Selleckchem	Cat#S1013
Protease Inhibitor Cocktail	Sigma	Cat#P9599
DUCHEFA Cellulase R-10	Melford Biolaboratories Limited	Cat#C8001.0010
EZ-Chemiluminescence Detection Kit for HRP	Geneflow	Cat#K1-0170
GFP-Trap MA magnetic beads	Chromotek	Cat#gtma-20
EZview Red Anti-c-Myc Affinity Gel	Sigma	Cat#E6654
EZview Red Protein A Affinity Gel	Sigma	Cat#P6486
c-Myc Peptide	Merck	Cat#M2435
GST	Ling et al ¹⁴	N/A
GST-SP1cyt	Ling et al ¹⁴	N/A
GST-SP1cyt-C330A	Ling et al ¹⁴	N/A
GST-SPL1cyt	This paper	N/A
GST-SPL1cyt-H308Y	This paper	N/A
GST-SPL2cyt	This paper	N/A
GST-SPL2cyt-H348Y	This paper	N/A
HA-ubiquitin	R&D systems-Boston Biochem	Cat#U-110-01M
human E1	Sigma	Cat#U5633
macerozyme R-10	Melford Biolaboratories Limited	Cat#M8002.0005
Percoll	Sigma	Cat#GE17-0891-01
qPCR BIO SyGreen Mix Hi-ROX	PCR Biosystems	Cat#PB20.12-20
SP1-YFP	Ling et al ¹⁴	N/A
SP1-Myc	Ling et al ¹⁶	N/A
SPL1-YFP	Ling et al ¹⁴	N/A
SPL1-HA	This paper	N/A

(Continued on next page)

Continued

REAGENT or RESOURCE	SOURCE	IDENTIFIER
SPL2-YFP	Ling et al ¹⁴	N/A
YFP-HA	Ling et al ¹⁴	N/A
SuperScript IV Reverse Transcriptase	Invitrogen	Cat#18090200
TNT T7 Quick for PCR DNA	Promega	Cat#L5540

Experimental models: Organisms/strains

<i>Arabidopsis</i> : <i>ppi1</i> : <i>ppi1-1</i>	Jarvis et al ²³	N/A
<i>Arabidopsis</i> : <i>sp1</i> : <i>sp1-1</i>	Ling et al ¹⁴	N/A
<i>Arabidopsis</i> : <i>sp1-1</i> : <i>sp1-1</i>	Arabidopsis Biological Resource Center	salk_064720
<i>Arabidopsis</i> : <i>sp1-2</i> : <i>sp1-2 (dal2-1)</i>	Arabidopsis Biological Resource Center	salk_024744
<i>Arabidopsis</i> : <i>sp1-3</i> : <i>sp1-3 (dal2-2)</i>	Arabidopsis Biological Resource Center	WiscDsLox383C6
<i>Arabidopsis</i> : <i>SP1-OX</i> : <i>SP1-OX</i>	Ling et al ¹⁴	N/A
<i>Arabidopsis</i> : <i>sp1-1 ppi1</i> : <i>sp1-1 ppi1-1</i>	Ling et al ¹⁴	N/A
<i>Arabidopsis</i> : <i>sp1-3 ppi1</i> : <i>sp1-3 ppi1-1</i>	Ling et al ¹⁴	N/A
<i>Arabidopsis</i> : <i>SP1-OX ppi1</i> : <i>SP1-OX ppi1-1</i>	Ling et al ¹⁴	N/A
<i>Arabidopsis</i> : <i>SPL1-OX ppi1</i> : <i>SPL1-OX ppi1-1</i>	Ling et al ¹⁴	N/A
<i>Arabidopsis</i> : <i>SPL2-OX sp1-3 ppi1</i> : <i>SPL2-OX sp1-3 ppi1-1</i>	This paper	N/A
<i>Arabidopsis</i> : <i>SPL2-KD ppi1</i> #1: <i>SPL2-KD ppi1-1</i> #1	This paper	N/A
<i>Arabidopsis</i> : <i>SPL2-KD ppi1</i> #2: <i>SPL2-KD ppi1-1</i> #2	This paper	N/A
<i>Arabidopsis</i> : <i>SPL2-KD</i> : <i>SPL2-KD</i>	This paper	N/A
<i>Arabidopsis</i> : <i>sp1-1 sp1-1</i> : <i>sp1-1 sp1-1</i>	This paper	N/A
<i>Arabidopsis</i> : <i>SPL2-OX</i> : <i>SPL2-OX</i>	This paper	N/A
<i>Arabidopsis</i> : <i>sp1-2 ppi1</i> : <i>sp1-2 ppi1-1</i>	This paper	N/A
<i>Arabidopsis</i> : <i>SPL1-OX ppi1</i> : <i>SPL1-OX ppi1-1</i>	This paper	N/A
<i>Arabidopsis</i> : <i>SP1-OX ppi1</i> > <i>ppi1</i> F1: <i>SP1-OX ppi1-1</i> > <i>ppi1-1</i> F1	This paper	N/A
<i>Arabidopsis</i> : <i>SPL1-OX ppi1</i> > <i>ppi1</i> F1: <i>SPL1-OX ppi1-1</i> > <i>ppi1-1</i> F1	This paper	N/A
<i>Arabidopsis</i> : <i>SP1-OX ppi1</i> > <i>SPL1-OX ppi1</i> F1: <i>SP1-OX ppi1-1</i> > <i>SPL1-OX ppi1-1</i> F1	This paper	N/A

Oligonucleotides

See Table S1 for oligonucleotides	N/A	N/A
-----------------------------------	-----	-----

Software and algorithms

Aida Image Analyzer	Raytest	http://www.elysia-raytest.com
MergeAlign	Collingridge and Kelly ⁴⁶ ; Katoh et al ⁴⁷	https://mergealign.appspot.com
IQ-TREE	Trifinopoulos et al ⁴⁸	http://iqtree.cibiv.univie.ac.at
ITOL	Letunic and Bork ⁴⁹	https://itol.embl.de
I-TASSER	Zhang ⁵⁰ ; Roy et al ⁵¹	https://zhanglab.ccmb.med.umich.edu/I-TASSER/
PyMOL	Schrödinger	https://pymol.org/2/
Fiji (ImageJ)	Schindelin et al ⁵²	https://imagej.nih.gov/ij/
RStudio	The R Foundation	https://www.r-project.org
Web MicroRNA Designer	Ossowski et al ²⁵ ; Schwab et al ²⁶	http://wmd3.weigelworld.org/cgi-bin/webapp.cgi

RESOURCE AVAILABILITY

Lead contact

Further information and requests for resources and reagents should be directed to and will be answered by the Lead Contact, R. Paul Jarvis (paul.jarvis@biology.ox.ac.uk).

Materials availability

Plasmids and plant lines generated in this study can be obtained through the Lead Contact.

Data and code availability

This study did not generate any unique datasets or code.

EXPERIMENTAL MODEL AND SUBJECT DETAILS

All *Arabidopsis thaliana* plants used in this study were of the Columbia-0 (Col-0) ecotype. Transgenic plant lines were generated by agrobacterium-mediated transformation. Seeds were either germinated on petri dishes containing Murashige and Skoog (MS) medium (4.3 g L⁻¹ MS basal salt mixture, 0.5% [w/v] sucrose, 0.05% [w/v] 2-[N-morpholino]ethanesulfonic acid [MES], pH adjusted to 5.7 with potassium hydroxide [KOH]; phyto-agar was added to a concentration of 0.65% [w/v] before sterilization by autoclaving at 110°C for 15 minutes), or on soil (Levington Advance Seed and Modular F2). Where necessary, 10 µg mL⁻¹ DL-phosphinothricin (Duchefa) was included in the MS medium for the selection of transformants. For in vitro growth, seeds were surface sterilized for 5 minutes with 70% (v/v) ethanol and 0.05% (v/v) Triton X-100, followed by an additional 10 minutes with 100% (v/v) ethanol before sowing. Plates were stratified in the dark at 4°C for a minimum of 2 days. Plants grown in vitro or on soil were kept under standard growth conditions at 22–24°C with a long-day photoperiod (16 hours light, 8 hours dark) of 120 µmol m⁻² s⁻¹ white light.

METHOD DETAILS

Physiological analysis

Chlorophyll content analysis of *Arabidopsis* seedlings was performed using a spectrophotometer following extraction with *N,N'*-dimethylformamide (DMF), as previously described.⁵³ For mature plants, chlorophyll levels were measured using a Konica-Minolta SPAD-502 meter with the recorded values converted into nmol per mg fresh weight using a published equation.⁵⁴

Induction of senescence by dark treatment was performed on equally-developed leaves of 28-day-old plants using previously described procedures.¹⁴ Photosynthetic performance (maximum photochemical efficiency of photosystem II, F_v/F_m) was recorded using a CF Imager chlorophyll fluorescence imaging system (Technologica, Essex, UK) as described previously.¹⁵

Generation of transgenic plant lines

To generate the *SPL2* cassette for the generation of *SPL2* overexpression (OX) lines, the full-length *Arabidopsis SPL2* coding sequence (CDS) was amplified by PCR from wild-type cDNA using the following primers: *SPL2*-cDNA-F, 5'-AAAAAGCAGGCTC CACTGTGCCGTGTGACCG-3'; and *SPL2*-cDNA-R, 5'-AGAAAGCTGGGTTATCGGTTACAAAATTTCTTCC-3'. All primers used in this study are listed in Table S1.

To prepare the artificial microRNA (amiRNA) cassette for the generation of *SPL2* knockdown (KD) lines, the original miR319a sequence in the pRS300 plasmid was replaced with an *SPL2* target sequence, essentially as described previously.²⁶ The following primers were designed using the Web MicroRNA Designer (WMD) platform²⁵ and used: *SPL2*amR1-I miR-s, 5'-GATACTAAG AGTAATATACGCGCTCTCTCTTTTGTATTCC-3'; *SPL2*amR1-II miR-a, 5'-GAGCGCGTATATTACTCTTAGTATCAAAGAGAATCAA TGA-3'; *SPL2*amR1-III miR*s, 5'-GAGCACGTATATTACACTTAGTTTCACAGGTCGTGATATG-3'; and *SPL2*amR1-IV miR*a, 5'-GA AACTAAGTGAATATACGTGCTCTACATATATATTCCT-3'.

The *SPL2* CDS and the *SPL2* amiRNA cassettes were each cloned into the cauliflower mosaic virus (CaMV) 35S-promoter-driven binary overexpression vector pB2GW7⁴⁴ using the Gateway cloning system (Invitrogen), generating the *SPL2*-OX and *SPL2*-KD constructs, respectively. The constructs were introduced into *Arabidopsis* wild-type, *sp1-3 ppi1*, or *ppi1* plants using the floral dip method.⁵⁵ At least 10 independent T1 lines were analysed per construct, and single-locus T2 lines showing a 3:1 segregation of resistance on selective medium were propagated for further analysis.

Characterization of mutant and transgenic plant lines

Analysis of gene expression by semi-quantitative or quantitative RT-PCR, analysis of protein levels by immunoblotting, and chloroplast isolation and protein import assays were all performed as described previously.^{15,45,56,57}

The primers used for semi-quantitative RT-PCR were: *SPL2*, 5'-AAAAAGCAGGCTCCATGTCTCGCCGGAGCGTG-3' and 5'-AGAAAGCTGGGTTCTAAGAGTAATATACACGCATAGAT-3'; and *elf4e1*, 5'-AAACAATGGCGGTAGAAGACACTC-3' and 5'-AAGATTGAGAGGTTTCAAGCGGTGTAAG-3'. The primers used for quantitative RT-PCR were: *SPL2*, 5'-ATGACCAAGGACAA GATGA-3' and 5'-ATGCCAACAGACACAATG-3'; and *ACTIN2*, 5'-TCAGATGCCCAAGTCTTGTTC-3' and 5'-CCGTACA GATCCTTCTGATATCC-3'.

Immunoblotting was performed using a standard procedure as described previously.^{15,57} Primary antibodies used to detect the chloroplast proteins were as follows: anti-atToc159,⁴² anti-atToc75-III,⁴¹ anti-atToc33,⁴³ anti-atTic110,⁴⁰ anti-atTic40,⁴¹ and anti-atStic1/Alb4.³⁹ Other primary antibodies employed in this study were: anti-Histone H3 (Abcam), anti-GFP (green fluorescent protein) (Sigma), anti-Myc (Abcam), and anti-HA (haemagglutinin) tag (Sigma). Anti-rabbit immunoglobulin G (IgG) conjugated with horseradish peroxidase (Abcam) was employed as the secondary antibody. Bands were detected using an EZ-Chemiluminescence Detection Kit for HRP (Geneflow), and recorded using an LAS-4000 imager (GE Healthcare). Band intensities were quantified using Aida Image Analyzer software (Raytest).

Immunoprecipitation

Isolation of protoplasts from the rosette leaves of 4-week-old wild-type plants, and their use for the transient expression of tagged proteins, was conducted as described previously.^{15,58} The *SPL1-HA* construct was generated by subcloning the *SPL1* coding sequence (CDS)¹⁴ into a modified p2GW7 plant expression vector providing a C-terminal hemagglutinin (HA) tag; and the *SPL2-YFP* construct used was generated by cloning the *SPL2* CDS (amplified using *SPL2*-CDS-F, 5'-AAAAAGCAGGCTCCATGTCCTCGCCGGAGCGTG-3'; and *SPL2*-nonstop-R, 5'-AGAAAGCTGGGTTAGAGTAATATACACGCATAG-3') into the pK7YWG2 binary vector.⁴⁴ The *SP1-YFP*, *SP1-Myc*, *SPL1-YFP* and *YFP-HA* constructs have been described previously.¹⁴ The proteasome inhibitor bortezomib (Selleckchem) was added to the protoplast culture medium after 15 hours of incubation following transfection, to a final concentration of 5 μ M; cultures were then incubated for an additional 4 hours before analysis.

Immunoprecipitation of the YFP fusion proteins was carried out using a previously described procedure,^{14,16} with minor modifications. Following cell lysis, total protein extracts were incubated with 25 μ L GFP-Trap MA magnetic beads (Chromotek) for 1 hour on a rotating mixer at 4°C. A MagJET separation rack (Thermo Fisher) was used to pellet the beads and any bound protein complexes. After four rounds of washing, each one with 500 μ L wash buffer (25 mM Tris-HCl, pH 7.5, 150 mM NaCl, 10% [v/v] glycerol, 1 mM EDTA, 0.5% [v/v] Triton-X100), the bound proteins were eluted by boiling in 2 \times protein loading buffer (60 mM Tris-HCl, pH 6.8, 10% [v/v] glycerol, 2% [w/v] sodium dodecyl sulphate [SDS], 0.05% [w/v] bromophenol blue, 0.1 M dithiothreitol [DTT]) for 5 minutes, and analysed by SDS-PAGE and immunoblotting.

Phylogenetic analysis

The amino acid sequences of the SP1, SPL1 and SPL2 homologues employed in the analysis were retrieved by using the *Arabidopsis thaliana* sequences as queries to perform BLASTP searches of the Phytozome,⁵⁹ Ensembl Plants,⁶⁰ and National Center for Biotechnology Information (NCBI) databases. All identified plant accessions with a complete RING domain sequence were retrieved and checked by performing reciprocal BLAST searches against the *A. thaliana* genome. Plant species that were represented by sequences truncated in the highly-conserved C3HC4 RING domain were not included in the analysis. The related human mitochondrial outer-membrane protein MULAN/MAPL (NM_024544) was included in the analysis as an outgroup. The sequences were aligned using MergeAlign,^{46,47} and phylogeny was inferred by maximum likelihood using the IQ-TREE⁴⁸ web server. The interactive Tree Of Life (iTOL) version 4 program⁴⁹ was used to visualise the tree.

Protein structural modelling

The protein structure models of the *A. thaliana* SP1 (residues 241–343), SPL1 (residues 240–338), and SPL2 (residues 288–383) cytosolic RING domains were predicted by submitting the corresponding amino acid sequences to the I-TASSER (Iterative Threading Assembly Refinement) online server.^{50,51} Predicted models with the highest confidence scores (C-scores) were selected and visualized using PyMOL (<https://pymol.org/2/>).

Transmission electron microscopy

Transmission electron microscopy (TEM) was performed on 4-week-old developmentally equivalent leaves as described previously,⁶¹ with several modifications as follows: 2 mm discs were excised from leaves using a biopsy punch, then cut in half with a scalpel. Leaf samples were cut in a droplet of primary fixative (2.5% [v/v] glutaraldehyde and 4% [v/v] paraformaldehyde [PFA] in 0.1 M sodium cacodylate buffer [SCB], pH 6.9) and fixed in a Leica AMW microwave processing unit at 37°C with five alternating 2-minute cycles of 20 W and 0 W power. The samples were then allowed to fix further at room temperature for ~5 hours in glass vials over-filled with primary fixative, and then left at 4°C overnight. Prior to secondary fixation, the overnight samples were washed four times, as follows: twice for 45 minutes and 30 minutes in 0.1 M SCB, pH 6.9; once for 30 minutes in 0.1 M SCB, pH 6.9, containing 50 mM glycine; and once for 20 minutes in 0.1 M SCB, pH 6.9. The samples were then incubated in secondary fixative (1% [v/v] osmium tetroxide in 0.1 M SCB, pH 6.9, containing 1.5% [w/v] potassium ferrocyanide) for 2 hours at 4°C, and for a further 50 minutes at room temperature, with rotation. The dehydration series was performed with ice-cold ethanol at 4°C with rotation, and following the final incubation in 100% ethanol the samples were transferred to ice-cold 100% acetone and incubated for 30 minutes at room temperature. Samples were infiltrated with epoxy resin as described,⁶¹ except that TAAB Hard Plus resin and acetone were used, and the samples were left an extra 24 hours in 100% resin before polymerization.

Chloroplast images were captured at the same magnification level using a Tecnai 12 TEM operated at 120 kV. Three samples per genotype were analysed, and at least ten different whole-chloroplast images per plant sample were recorded (a total of 30 chloroplasts per genotype). Chloroplast cross-sectional area was estimated using Fiji, a distribution of the open-source software package ImageJ.⁵²

Recombinant proteins and in vitro ubiquitination assays

The expression and purification of GST, GST-SP1cyt (residues 244–343), GST-SP1cyt-C330A (Cys330-to-Ala), GST-SPL1cyt (residues 241–338), GST-SPL1cyt-H308Y (His308-to-Tyr), GST-SPL2cyt (residues 289–383), and GST-SPL2cyt-H348Y (His348-to-Tyr) followed a procedure that has been described previously.¹⁴ The primers used for the generation of the *SPL*-related constructs were: *SPL1cyt*, 5'-GGGGACAAGTTTGTACAAAAAAGCAGGCTCCGTGATTGAATATATTCTA-3' and 5'-GGGGACCACTTTGTACAA GAAAGCTGGGTTTCAATGGCGGTAAATTTTC-3'; and *SPL2cyt*, 5'-GGGGACAAGTTTGTACAAAAAAGCAGGCTCCGTGCTGTCA GGACCTGGAA-3' and 5'-AGAAAGCTGGGTTCTAAGAGTAATATACACGCATAGAT-3'. The RING mutant *SPL* constructs were generated by combined overlap-extension PCR in vitro⁶² using these additional primers: *SPL1-H308Y*, 5'-GAGTGTGGTTATAT GTGCTG-3' and 5'-CAGCACATATAACCACACTC-3'; and *SPL2-H348Y*, 5'-CCTGCGTTTATCCCTGTGGATATGTAGTATG-3' and 5'-CACATCGCCTGCAACATACTACATATCCACAG-3'. The *GST*, *GST-SP1cyt* and *GST-SP1cyt-C330A* constructs have all been described before.¹⁴

Ubiquitination assays employed a method described previously.¹⁴ An alternative E2 enzyme, human Ubch5b (Boston Biochem), was also employed in place of 6xHis-tagged AtUBC8 in some assays. For the ubiquitination experiments containing two recombinant E3 ligases, the proteins were mixed in different amount ratios (1:2, 1:4 and 1:8) in the same 30 μ L reaction.

QUANTIFICATION AND STATISTICAL ANALYSIS

Statistical analysis was carried out using RStudio Version 1.2.5019. The numbers of samples analysed, and the reference group used, are specified in the figure legends. The p values were derived from Student's t-test analysis (two-tailed) of the means of the indicated genotypes (ns, not significant at $p > 0.05$; *, significant at $p < 0.05$; **, significant at $p < 0.01$; ***, significant at $p < 0.001$, ****, significant at $p < 0.0001$)